Mon. Not. R. Astron. Soc. **000**, 1–11 (2010) Printed 6 March 2012 (MN LATEX style file v2.2)

Quantifying the Universality of the Stellar Initial Mass Function in Old Star Clusters

Nathan Leigh[1,2], Stefan Umbreit[3,4], Alison Sills[1], Christian Knigge[5], Guido de Marchi[2], Evert Glebbeek[1,6], Ata Sarajedini[7⋆]

[1] *Department of Physics and Astronomy, McMaster University, 1280 Main St. W., Hamilton, ON, L8S 4M1, Canada*
[2] *European Space Agency, Space Science Department, Keplerlaan 1, 2200 AG Noordwijk, The Netherlands*
[3] *Center for Interdisciplinary Exploration and Research in Astrophysics (CIERA), Northwestern University, Evanston, IL 60208, USA*
[4] *Department of Physics and Astronomy, Northwestern University, Evanston, IL 60208, USA*
[5] *School of Physics and Astronomy, University of Southampton, Highfield, Southampton, SO17 1BJ, United Kingdom*
[6] *Department of Astrophysics/IMAPP, Radboud University Nijmegen, P.O. Box 9010, 6500 GL Nijmegen, The Netherlands*
[7] *Department of Astronomy, University of Florida, Gainesville, FL 32611, USA*

6 March 2012

ABSTRACT

We present a new technique to quantify cluster-to-cluster variations in the observed present-day stellar mass functions of a large sample of star clusters. Our method quantifies these differences as a function of both the stellar mass and the total cluster mass, and offers the advantage that it is insensitive to the precise functional form of the mass function. We applied our technique to data taken from the Advanced Camera for Surveys Survey for Globular Clusters, from which we obtained completeness-corrected stellar mass functions in the mass range 0.25-0.75 $M_\odot$ for a sample of 27 clusters. The results of our observational analysis were then compared to Monte Carlo simulations for globular cluster evolution spanning a range of initial mass functions, total numbers of stars, concentrations, and virial radii.

We show that the present-day mass functions of the clusters in our sample can be reproduced by assuming an universal initial mass function for all clusters, and that the cluster-to-cluster differences are consistent with what is expected from two-body relaxation. A more complete exploration of the initial cluster conditions will be needed in future studies to better constrain the precise functional form of the initial mass function. This study is a first step toward using our technique to constrain the dynamical histories of a large sample of old Galactic star clusters and, by extension, star formation in the early Universe.

Key words: globular clusters: general – stellar dynamics – stars: statistics – methods: statistical – stars: formation – stars: low-mass.

1 INTRODUCTION

It is now thought that most, if not all, of the stars in our Galaxy were born in star clusters (e.g. Lada & Lada 1995, 2003; McKee & Ostriker 2007). And yet, there remain several key details of the star formation process that are still not understood. Part of the problem lies in the fact that populations of young stars are typically hidden by a dense veil of optically-thick gas and dust. This prevents the escape of most of the light produced by infant stars, and often renders these regions difficult to observe (e.g. Grenier, Casandijan & Terrier 2005; Lada, Alves & Lombardi 2007). Most of these clusters are sparsely populated and are of relatively low mass ($M \lesssim 10^4$ $M_\odot$) (e.g. Lada 1985). They are also very young since clusters of such low mass are unlikely to survive for more than 1 Gyr (e.g. Portegies Zwart, McMillan & Gieles 2010).

At the other end of the cluster mass spectrum, most massive star clusters ($M \gtrsim 10^4$ $M_\odot$) in our Galaxy tend to be at least a few Gyrs old, and in many cases are nearly as old as the Universe itself (e.g. Harris 1996, 2010 update; De Angeli et al. 2005). These clusters have the advantage that they are no longer obscured by the primordial gas from which they formed, however they are a dynamically active environment. As a result, the conditions present at

⋆ E-mail: leighn@mcmaster.ca (NL); s-umbreit@northwestern.edu (SU); asills@mcmaster.ca (AS1); christian@astro.soton.ac.uk (CK); e.glebbeek@astro.ru.nl (EG); gdemarchi@esa.rssd.int (GD); ata@astro.ufl.edu (AS2)

the time of their formation have now been largely erased (e.g. Portegies Zwart et al. 2001; Hurley et al. 2005; Murray 2009). This presents a considerable challenge for studying star formation in the regime of cluster masses and metallicities that characterize Milky Way globular clusters. This is unfortunate since these old star clusters contain the fossil record of a very early episode of star formation in the Universe, and are the only means of studying it locally in massive star clusters.

One of the primary observational tests for star formation theories is the stellar initial mass function (IMF). Current observational evidence suggests that the IMF is very similar in different regions of our Galaxy, including the disk and young star clusters (e.g. Elmegreen 1999; Kroupa et al. 2011). However, this is still being debated throughout the literature (e.g. Scalo 1998; Parravano, McKee & Hollenbach 2011). Different star formation theories tend to predict different IMFs. These vary with the properties of the gas clouds from which the stars are born, including density, temperature and composition (e.g. Elmegreen 2001; Bonnell, Larson & Zinnecker 2007; McKee & Ostriker 2007; Kroupa et al. 2011).

Given the sensitive nature of the observations, a large sample of IMFs spanning the entire range of cluster properties exhibited by star clusters in the Milky Way, including total mass and chemical composition, has yet to be compiled. This is a sorely needed step in order to advance our understanding of star formation by providing direct comparisons between observations and theoretical predictions. This is especially true of massive, metal-poor star clusters since we are particularly lacking observations of IMFs in this regime of cluster masses and metallicites (e.g. McKee & Ostriker 2007; Portegies Zwart, McMillan & Gieles 2010). Important steps in this direction were recently taken by De Marchi, Paresce & Portegies Zwart (2010) and Paust et al. (2010), who studied the present-day mass functions of a large sample of Galactic clusters and considered the effects of the cluster dynamics in modifying them from their primordial forms.

For the very first time, the Advanced Camera for Surveys (ACS) Survey for Globular Clusters has provided photometry for a large sample of Milky Way globular clusters (GCs) that reaches down to unprecedented faint magnitudes. This offers a large sample of current stellar mass functions spanning the stellar mass range $\approx 0.2 - 0.8$ M$_{\odot}$. All of the clusters are massive and very old, with total masses and ages ranging from $\approx 10^4$ - 10^6 M$_{\odot}$ and $\approx$ 10-12 Gyrs, respectively (Harris 1996, 2010 update; De Angeli et al. 2005). This has allowed significant time for their stellar mass functions to have been modified from their primordial forms due to both stellar evolution and stellar dynamics. However, most of the processes responsible for this evolution are now largely understood. Therefore, in principle, it is possible to use current observations of old star clusters together with theoretical models for their evolution to extrapolate backwards in time and indirectly probe their IMFs.

For most of the life of a massive star cluster, two-body relaxation is the dominant physical mechanism driving its evolution (e.g. Henon 1960; Spitzer 1987; Heggie & Hut 2003; Gieles, Heggie & Zhao 2011). The term describes the cumulative effects of long-range gravitational interactions that occur between pairs of stars, which act to alter their orbits within the cluster. This results in a phenomenon known as mass segregation, which is the tendency for heavier stars to accumulate in the central cluster regions and low-mass stars to be dispersed to wider orbits. This mechanism also causes stars to escape from their host cluster, with the probability of ejection increasing with decreasing cluster mass. Therefore, two-body relaxation acts to slowly modify the distribution of stellar masses within clusters, and can cause very dynamically evolved clusters to appear severely depleted of their low-mass stars. Evidence in favour of this process having actually occurred in real star clusters has been reported by several authors (e.g. von Hippel & Sarajedini 1998; De Marchi, Paresce & Portegies Zwart 2010).

A number of theoretical studies have been conducted to learn how the evolution of the stellar mass function (MF) in GCs is affected by two-body relaxation, stellar evolution, disc shocking, and tidal effects from the Galaxy (see Baumgardt & Makino (2003) for a detailed review). In the absence of these effects, we expect the MF to continually rise toward lower stellar masses. By performing a series of N-body simulations, Vesperini & Heggie (1997) showed that tidal effects from the Galaxy, disc shocking, and a higher initial central concentration all act to increase the rate of stellar evaporation, and accelerate the depletion of preferentially low-mass stars. These results were confirmed and built upon by Baumgardt & Makino (2003) who showed that the depletion of low-mass stars can be sufficiently dramatic to change the sign of the slope of the MF at the low-mass end. Interestingly, these results were not supported by the observational study of De Marchi, Paresce & Pulone (2007). These authors analyzed the MFs in a sample of 20 Galactic GCs, and found that the slope of the MF decreases with increasing central concentration. They argued that this contradicts what is expected from theory since two-body relaxation is responsible both for increasing the central density and flattening the MF at the low-mass end. In an effort to explain this, they suggested that many of the clusters in their sample could be post-core collapse, and therefore had much higher central densities in the past. Alternatively, Marks, Kroupa & Baumgardt (2008) argued that this can be explained by residual gas-expulsion from initially mass segregated clusters (e.g. Tutukov 1978), and cautioned that unresolved binaries could also be contributing.

Several theoretical studies have also been conducted to study the dynamical histories of individual globular clusters (e.g. Heggie & Giersz 2008, 2009). For example, Zonoozi et al. (2011) recently performed the first ever direct N-body simulations of a Milky Way (MW) GC over its entire lifetime. This was done for the distant GC Palomar 14, which has an unusually low-density and large radius. The emphasis of this paper is to use the ensemble information of many GCs to learn about the universality of the IMF in old massive star clusters. Individual cases, in particular Pal 14, are often chosen for their peculiar characteristics and may not be representative of the bulk of the GCs in the MW.

In this paper, we present a new technique to quantify cluster-to-cluster variations in the observed stellar mass functions of a large sample of clusters spanning a diverse range of properties. Our method offers the advantage that it is insensitive to the precise functional form of the MF. We have applied it to a sample of 27 MFs taken from the ACS Survey for Globular Clusters (Sarajedini et al. 2007).

Can the present-day MFs be explained by an universal IMF and stellar evaporation induced by two-body relaxation? Or are cluster-specific IMFs needed to reproduce the observed MFs? To address these questions, we compared the results of our observational analysis to 268 Monte Carlo simulations for GC evolution. The models spanned a range of initial masses, virial radii, central concentrations and IMFs. Therefore, by evolving all of these models to the current ages of the GCs in our sample and comparing the resulting MFs to the present-day observed ones, we have quantified the dynamical evolution of the MFs in our observed sample. This has allowed us to take the first steps toward constraining both the exact functional forms of the IMFs of MW GCs and the conditions present at the time of their formation.

In Section 2, we present our sample of observed stellar mass functions and describe both our technique for analyzing the observations and the models for globular cluster evolution to which they are compared. The results of our analysis of the ACS observations are presented in Section 3, along with an example comparison between the observations and the models. This example demonstrates how our method can be used to compare a large number of observed MFs to analogous samples of simulated MFs. Finally, we discuss in Section 4 the implications of our results for the conditions present in our observed clusters at the time of their formation and the role played by two-body relaxation in modifying the stellar MF to its present-day form.

2 METHOD

In this section, we describe how we acquired our sample of mass functions from the ACS data, as well as the Monte Carlo simulations for globular cluster evolution used for comparison to the observations.

2.1 The Data

The data used in this study was taken from the sample of 35 MW GCs used in Leigh, Sills & Knigge (2011), which was in turn taken from the ACS Survey for Globular Clusters (Sarajedini et al. 2007).[1] The ACS Survey provides unprecedented deep photometry in the F606W ($\approx$ V) and F814W ($\approx$ I) filters that is nearly complete down to $\approx$ 0.2 $M_\odot$. In other words, the colour-magnitude diagrams (CMDs) extend reliably from the horizontal branch all the way down to about 7 magnitudes below the main-sequence turn-off (MSTO). A list of the GCs used in this study is shown in Table 1 along with their core radii (r_c), half-mass radii (r_h), central luminosity densities (ρ_0), and central concentration parameters (c). These were taken directly from Harris (1996, 2010 update), with the exception of the core and half-mass radii. The latter quantities are given in parsecs and were calculated using the distance modulii and extinction corrections provided in Harris (1996, 2010 update).

Each cluster was centred in the ACS field, which extends out to several core radii from the cluster centre in most cases. Coordinates for the cluster centres were taken from Goldsbury et al. (2010). These authors found their centres by fitting a series of ellipses to the density distributions within the inner 2' of the cluster centre, and computing an average value.

[1] The data can be found at http://www.astro.ufl.edu/~ata/public_hstgc/.

Table 1. List of globular clusters and their structural parameters

Cluster ID	Alternate ID	r_c (in pc)	r_h (in pc)	ρ_0 (in $L_\odot$ pc^{-3})	c
104	47 Tuc	0.47	4.11	4.88	2.07
1261		1.66	3.22	2.99	1.16
2298		0.97	3.08	2.90	1.38
4147		0.51	2.70	3.63	1.83
4590	M 68	1.73	4.51	2.57	1.41
5024	M 53	1.82	6.80	3.07	1.72
5272	M 3	1.10	6.84	3.57	1.89
5286		0.95	2.48	4.10	1.41
5904	M 5	0.96	3.85	3.88	1.73
5927		0.94	2.46	4.09	1.60
5986		1.43	2.97	3.41	1.23
6093	M 80	0.44	1.78	4.79	1.68
6121	M 4	0.59	2.18	3.64	1.65
6171	M 107	1.04	3.21	3.08	1.53
6205	M 13	1.29	3.51	3.55	1.53
6218	M 12	1.11	2.49	3.23	1.34
6254	M 10	0.98	2.49	3.54	1.38
6304		0.36	2.43	4.49	1.80
6341	M 92	0.63	2.45	4.30	1.68
6535		0.71	1.68	2.34	1.33
6584		1.02	2.86	3.33	1.47
6637	M 69	0.84	2.15	3.84	1.38
6779	M 56	1.21	3.02	3.28	1.38
6838	M 71	0.74	1.96	2.83	1.15
6934		1.00	3.14	3.44	1.53
6981	M 72	2.28	4.60	2.38	1.21
7089	M 2	1.08	3.56	4.00	1.59

2.2 Measuring the Stellar Mass Function

First, we used the available photometry to obtain estimates for the masses of the stars in our sample. To do this, we fit theoretical isochrones taken from Dotter et al. (2007) to the CMDs of every cluster. Each isochrone was generated using the metallicity and age of the cluster, and fit to its CMD using the corresponding distance modulus and extinction provided in Dotter et al. (2010). The MSTO was then defined using our isochrone fits by selecting the bluest point along the main-sequence (MS).

We considered five stellar mass bins along the MS. These ranged from 0.25 - 0.75 $M_\odot$ in increments of 0.1 $M_\odot$. This range was chosen to help ensure complete sampling in all bins since the lowest MSTO mass in our sample corresponds to $\approx$ 0.75 $M_\odot$, and the photometric errors remain small ($\lesssim$ 0.05 mag) within the magnitude range for each stellar mass bin in every cluster. We obtained number counts for all stellar mass bins in the annulus $r_c < r < 2r_c$, where r is the distance from the cluster center. This reduced our sample size by five clusters since the spatial coverage offered by the ACS field of view is incomplete in these cases.

We obtained completeness corrections for each stellar mass bin in the annulus immediately outside the core ($r_c < r < 2r_c$). This was done using the results of artificial star

Table 2. Completeness-corrected number counts for all five stellar mass bins in the annulus $r_c < r < 2r_c$

Cluster ID	MS1 (0.65 - 0.75 $M_\odot$)	MS2 (0.55 - 0.65 $M_\odot$)	MS3 (0.45 - 0.55 $M_\odot$)	MS4 (0.35 - 0.45 $M_\odot$)	MS5 (0.25 - 0.35 $M_\odot$)
104	15113	16056	–	–	–
1261	4652	4840	4747	4647	4441
2298	1022	865	828	673	595
4147	525	355	257	154	100
4590	2830	3179	3793	4477	5543
5024	9773	9626	9725	8114	5859
5272	9763	10447	12097	12886	14339
5286	9394	8330	6436	2765	941
5904	5382	6726	9226	–	–
5927	4304	4208	5244	6043	–
5986	10328	10936	12070	13012	13635
6093	4356	2658	–	–	–
6121	1111	879	–	–	–
6171	1207	1049	968	1064	–
6205	11757	13012	16176	–	–
6218	2480	2337	2348	2589	–
6254	4631	4826	5375	6394	7342
6304	1806	1941	–	–	–
6341	4127	4019	3771	2456	–
6535	292	200	188	143	134
6584	3083	3330	3624	3880	4498
6637	3166	3192	3710	3818	1714
6779	3273	2941	2983	3047	3088
6838	592	634	654	–	–
6934	2615	2416	2228	1836	1302
6981	2731	2774	2914	2865	2847
7089	12549	12388	10113	3458	–

tests taken from Anderson et al. (2008). Number counts for each mass bin were then multiplied by their corresponding completeness corrections. We did not include core number counts in our analysis since our completeness corrections begin to exceed 50% somewhere inside the core for every cluster in our sample. This is due to crowding and the high central surface brightnesses at the centres of our clusters. We have entirely removed three clusters from our original sample used in Leigh, Sills & Knigge (2011), namely NGC 1851, NGC 5139, and NGC 6652. This is because their completeness corrections exceeded 50% in every mass bin in the annulus immediately outside the core. We also removed additional clusters from our samples for the lowest three mass bins whenever their completeness corrections exceeded 50%. These clusters typically had the highest MSTO masses. In total, this left us with 27, 27, 23, 20, and 15 clusters in each of the five mass bins, in order of decreasing stellar mass. The completeness-corrected number counts for each stellar mass bin have been provided in Table 2.

The field of view of the ACS images is about 200" on a side, which gives physical scales ranging between 1.5 and 16 pc (for the closest and furthest clusters in our sample). Based on this, we expect foreground contamination by field stars to be negligible for most of the clusters in our sample given their current locations in the Galaxy. For example, Da Costa (1982) considered star count data in a similar area and over a comparable range of stellar masses for three nearby globular clusters. The author found that the corrections resulting from field contamination were always less than 10% over nearly the entire range of stellar masses we are considering.

2.3 Weighted Lines of Best-Fit

In order to quantify cluster-to-cluster differences in the present-day stellar mass functions of the clusters in our sample, we obtained lines of best-fit for (the logarithm of) the number of stars belonging to each stellar mass bin versus (the logarithm of) the total number of stars spanning all five mass bins, which provides a proxy for the total cluster mass. This can be written:

$$\log N_{bin,i} = \gamma_i \log\left(\frac{N_{tot}}{10^3}\right) + \delta_i, \quad (1)$$

where $N_{bin,i}$ is the number of stars belonging to mass bin i, N_{tot} is the total number of stars spanning all five mass bins, and γ_i and δ_i are both constants.

Our motivation for adopting this technique is as follows. If the fraction of stars belonging to each mass bin, or $f_{bin,i} = N_{bin,i}/N_{tot}$, is constant for all cluster masses, then we would expect $N_{bin,i}$ to scale linearly with N_{tot}. Or, equivalently, $\gamma_i \approx 1$ in Equation 1. However, if there is any systematic dependence of $f_{bin,i}$ on the total cluster mass, then we should find that $N_{bin,i}$ does *not* scale linearly with N_{tot}. In log-log space, the slope of the line of best-fit for stellar mass bin i should be less than unity (i.e. $\gamma_i < 1$) if $f_{bin,i}$ systematically decreases with increasing cluster mass. Conversely, we expect $\gamma_i > 1$ if $f_{bin,i}$ systematically increases with increasing cluster mass. This means that, for a sample of clusters with a wide range of total masses, we expect $\gamma_i < 1$ for the highest mass stars and $\gamma_i > 1$ for the lowest mass stars. This is because clusters lose preferentially low-mass stars due to two-body relaxation, and this process operates the fastest in lower mass clusters.

Equation 1 quantifies the number of stars belonging to each stellar mass bin as a function of the total cluster mass. More generally, it provides a means of quantifying cluster-to-cluster differences in the stellar mass function as a function of both the stellar mass and the total cluster mass.

The lines of best-fit have been weighted by adopting uncertainties for the number of stars in each mass bin using Poisson statistics. Uncertainties for the slopes (i.e. for γ_i in Equation 1) were found using a bootstrap methodology in which we generated 1,000 fake data sets by randomly sampling (with replacement) number counts from the observations. We obtained lines of best fit for each fake data set, fit a Gaussian to the subsequent distribution and extracted its standard deviation.

Table 3. Initial Model Parameters

Parameter	Initial Values
IMF slope (α)	1.3, 0.4, 0.0, -0.4
Number of Stars	1e5, 2e5, 4e5, 6e5, 8e5, 1e6, 2e6, 4e6
Concentration (W_0)	5.0, 5.5, 6.0, 6.5, 7.0
Virial Radius (in pc)	3, 4, 5

2.4 Monte Carlo Models

We have generated 268 Monte Carlo simulations for globular cluster evolution spanning a range of initial total numbers of stars, concentrations, virial radii and IMFs. The models realistically take into account both stellar and binary evolution, and track both short- and long-range gravitational interactions between both single and binary stars. Detailed explanations concerning the development of these models can be found in Joshi, Rasio & Portegies Zwart (2000), Joshi, Nave & Rasio (2001), Fregeau et al. (2003), Fregeau & Rasio (2007), and Chatterjee et al. (2010).

For every combination of initial concentration (W_0), virial radius (r_{vir}) and IMF slope (α in Equation 2), we generated a series of models with different initial total numbers of stars (i.e. total cluster masses). We adopted an IMF of the form:

$$\frac{dN}{dm} = \beta m^{-\alpha}, \quad (2)$$

where α and β are constants. This was taken from Kroupa (2001), who fit a three-part power-law to this function with $\alpha = 2.3$ for $0.50 < m/M_\odot < 1.00$, $\alpha = 1.3$ for $0.08 < m/M_\odot < 0.50$, and $\alpha = 0.3$ for $0.01 < m/M_\odot < 0.08$. We varied α only in the stellar mass range $0.08 < m/M_\odot < 0.50$.

Each model run was evolved for a period of 12 Gyrs, which roughly coincides with the ages of the clusters in our sample (e.g. De Angeli et al. 2005; Marin-Franch et al. 2009). The resulting collection of simulations spanned roughly the same range of total masses as our observed sample. The initial cluster parameters considered in this paper are shown in Table 3. With this suite of simulations, we have only scratched the surface in terms of exploring the total initial parameter space that could be relevant to the GCs in our observed sample. However, our goal in this paper is to demonstrate the strength of our technique for quantifying cluster-to-cluster differences in the observed present-day MFs, and to show by example how our method can be used to compare a large number of observed MFs to analogous samples of simulated MFs. We defer a more complete exploration of the total possible parameter space of initial conditions to a future paper.

The simulated clusters were placed on circular orbits at a distance of 4 kpc from the Galactic centre, and the resulting tidal effects from the Galaxy were accounted for. We note that these effects are reduced by adopting a smaller initial virial radius. The effects of tides were typically small in all but those models for which both the initial mass and concentration were very low, which agrees with the results of previous studies (e.g. Vesperini & Heggie 1997). We assumed a metallicity of $Z = 0.001$ for all simulated clusters. This roughly agrees with what is typically observed in Galactic GCs (e.g. Harris 1996, 2010 update), and primarily affects the rate of stellar mass loss due to winds early on in

the cluster lifetime when massive stars are still present (e.g. Chernoff & Weinberg 1990). Although this does affect the rate of dynamical evolution, the effect should be very similar from cluster-to-cluster for the initial conditions considered in this paper. This is because the mass loss that occurs early on in the cluster lifetime due to stellar evolution has the greatest impact on clusters with very low initial concentrations, and can significantly reduce the time for cluster dissolution in these cases. However, Baumgardt & Makino (2003) showed that this effect is not severe for the range of initial concentrations (W_0 = 5 - 7) considered here. Finally, we assumed an initial global binary fraction of 10% for all model runs using the same binary orbital parameter distributions as adopted in Chatterjee et al. (2010). We will return to these assumptions in Section 4.

We generated simulated CMDs for every model run by converting the bolometric luminosity of every star to its corresponding magnitude in the ACS F814W band. This was done using the colour conversion routine of Pols et al. (1998), which uses the spectral libraries of Lejeune, Cuisinier & Buser (1997) and Lejeune, Cuisinier & Buser (1998). For binary stars, the magnitudes of the components were combined in order to position them in the CMD as single objects.

Observations of star clusters are projected onto the plane of the sky, whereas the output from our models provides only a 3-D distance from the cluster centre for every single and binary star. Therefore, it was necessary to convert these 3-D distances to corresponding 2-D values. This was done by randomly varying the component along the line-of-sight to the cluster, and using the 3-D distance to calculate a 2-D value. Using these projected 2-D distances from the cluster centre, we also generated surface brightness profiles for every model run and re-calculated a 2-D core radius (defined as the distance from the cluster centre at which the surface brightness falls to half its central value). These 2-D core radii were then used to count the number of objects (i.e. single and binary stars) belonging to each stellar mass bin located within the annulus immediately outside the core (i.e. $r_c < r < 2r_c$).

2.5 Comparing the Observed and Simulated Present-Day Mass Functions

For every combination of initial concentration, virial radius, and IMF slope, the different runs corresponding to different initial numbers of stars were grouped together. This gave us a sample of MFs spanning a range of total cluster masses for every combination of initial conditions. The selection criteria described in Section 2.2 was then applied to each model, and lines of best-fit were found for each stellar mass. The slopes of these lines of best-fit (i.e. γ_i in Equation 1) were then compared to the corresponding observed slopes for every stellar mass, and both the chi-squared value and the probability that the two samples (i.e. the observed γ_i's for all five mass bins and a given set of theoretically-derived γ_i's for all mass bins) are drawn from the same distribution were found.

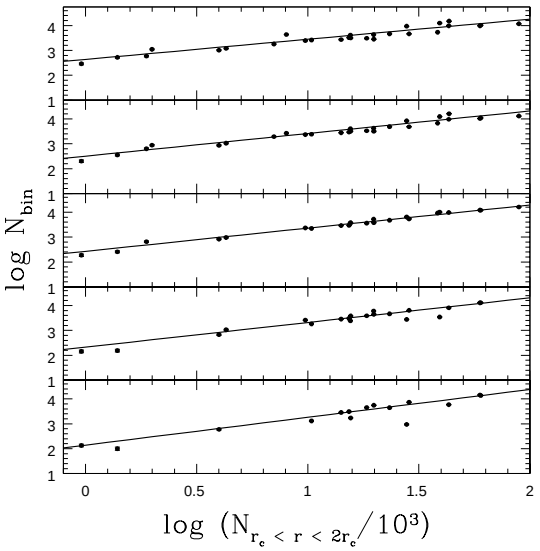

Figure 1. The logarithm of the number of stars belonging to each stellar mass bin (N_{bin}) as a function of the logarithm of the total number of stars spanning all five mass bins in the annulus immediately outside the core ($N_{r_c<r<2r_c}$). In descending order from top to bottom, the plots correspond to number counts in the mass ranges 0.65 - 0.75 $M_\odot$ (MS1), 0.55 - 0.65 $M_\odot$ (MS2), 0.45 - 0.55 $M_\odot$ (MS3), 0.35 - 0.45 $M_\odot$ (MS4), and 0.25 - 0.35 $M_\odot$ (MS5). Lines of best fit are shown for each mass bin by solid lines.

Table 4. Lines of Best Fit for $\log N_{bin,i} = (\gamma \pm \Delta\gamma)\log(N_{tot}/10^3) + (\delta \pm \Delta\delta)$

Stellar Mass	$\gamma \pm \Delta\gamma$; $\delta \pm \Delta\delta$
MS1 (0.65-0.75 $M_\odot$)	0.81 ± 0.09; 2.64 ± 0.12
MS2 (0.55-0.65 $M_\odot$)	0.91 ± 0.09; 2.50 ± 0.10
MS3 (0.45-0.55 $M_\odot$)	0.93 ± 0.03; 2.43 ± 0.04
MS4 (0.35-0.45 $M_\odot$)	0.99 ± 0.05; 2.33 ± 0.08
MS5 (0.25-0.35 $M_\odot$)	1.12 ± 0.11; 2.14 ± 0.17

3 RESULTS

In this section, we present the results of both our observational analysis and its comparison to the models.

3.1 Observational Analysis

We have plotted the logarithm of the number of stars in each stellar mass bin versus the logarithm of the total number of stars spanning all five mass bins in Figure 1. The slopes and y-intercepts for the weighted lines of best-fit performed for each of these relations provided values for γ_i and δ_i in Equation 1. These are shown in Table 4, along with their corresponding uncertainties ($\Delta\gamma$ and $\Delta\delta$). Each table entry has been provided in the form ($\gamma \pm \Delta\gamma$; $\delta \pm \Delta\delta$). The values for γ_i have also been plotted in Figure 2.

As shown in Figure 2, γ_i tends to systematically increase with decreasing stellar mass. The uncertainty for γ_i is the

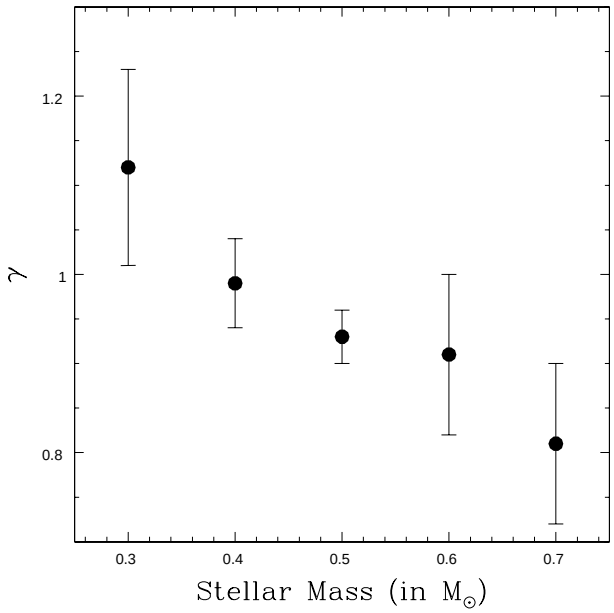

Figure 2. Slopes for the lines of best-fit, given by γ_i in Equation 1, plotted as a function of stellar mass.

highest for the lowest mass bin (MS5 in Table 4). This is because the photometric errors are the highest at these dim magnitudes. However, the errors are consistently at most $\approx$ 10% of the width in magnitude of their corresponding mass bin.

In an attempt to improve upon these statistics, we have also calculated reduced chi-squared values with added intrinsic dispersion for the relations for each mass bin. That is, for each mass bin we added a constant term to the uncertainty for each data point, found the uncertainty that yielded a reduced chi-squared of one, and looked at the subsequent effects on the uncertainties for the line of best-fit. Based on this, we appear to be slightly over-estimating the uncertainties for the MS1, MS2 and MS3 mass bins using our bootstrap approach, and slightly under-estimating them for the MS4 and MS5 bins.

The change in the distribution of stellar masses as a function of the total cluster mass can be illustrated using pie charts, as shown in Figure 3. Using the values for γ_i and δ_i provided in Table 4, we have generated pie charts for three total numbers of stars (spanning all five mass bins), namely $N_{tot} = 10^5$, 10^4, 10^3 (from top to bottom in Figure 3). As is clear, low-mass stars become more and more preferentially depleted with decreasing total cluster mass.

From top to bottom, the pie charts can be interpreted as depicting the evolution of the stellar mass function with increasing dynamical age. This can be understood as follows. The inverse of the half-mass relaxation time can be used as a proxy for the rate of two-body relaxation throughout the entire cluster. The half-mass relaxation time ranges from several million years to the age of the Universe or longer, and is approximated by (Spitzer 1987):

$$t_{rh} = 1.7 \times 10^5 [r_h(pc)]^{3/2} N^{1/2} [m/M_\odot]^{-1/2} years, \quad (3)$$

where r_h is the half-mass radius (i.e. the radius enclosing half the mass of the cluster), N is the total number of stars within r_h and m is the average stellar mass. Simulations have shown that r_h changes by a factor of at most a few over the course of a cluster's lifetime (Henon 1973; Murray 2009). The GCs that comprise the ACS sample show a range of masses spanning roughly 3 orders of magnitude (10^4-10^6 $M_\odot$), and have comparably old ages ($\approx$ 10-12 Gyrs) (De Angeli et al. 2005; Marin-Franch et al. 2009). Moreover, their half-mass radii typically differ by less than a factor of 2 (see Table 1). Therefore, Equation 3 suggests that the total cluster mass provides a rough proxy for the degree of dynamical evolution due to two-body relaxation. In other words, the effects of two-body relaxation on the evolution of the stellar mass function should be the most pronounced in the least massive clusters in the ACS sample (e.g. De Marchi, Paresce & Pulone 2007; Baumgardt, De Marchi & Kroupa 2008; Kruijssen & Mieske 2009). Said another way, dynamical age increases with decreasing cluster mass. Therefore, Figure 3 shows that our results are consistent with the general picture that two-body relaxation is the cause of the observed depletion of low-mass stars in low-mass clusters, as opposed to some unknown feature of the star formation process.

3.2 Theoretical Analysis

In this section, we compare the results of our observational analysis to 268 Monte Carlo simulations for globular cluster evolution spanning a range of initial conditions.

Figure 4 shows a comparison between all five γ_i values found from the observed MFs and the corresponding model γ_i values for every combination of initial conditions. As is clear, the agreement is excellent for nearly every combination of initial IMF, concentration and virial radius. This was confirmed by our chi-squared values, and the probability that the observed and model γ_i's are drawn from the same distribution exceeded 64% for all comparisons.

Our results suggest that a Kroupa IMF (i.e. $\alpha = 1.3$ in Equation 2) typically gives the best agreement with the observations. Every set of models with this IMF yielded a probability greater than 93% that the observed and model γ_i's are drawn from the same distribution. Our results also appear to be relatively insensitive to the initial concentration and virial radius. This agrees with what was found by Vesperini & Heggie (1997) and Baumgardt & Makino (2003) given the limited ranges we have explored for these parameters.

4 SUMMARY & DISCUSSION

In this paper, we have presented a new technique to quantify cluster-to-cluster variations in a large sample of observed stellar mass functions. Our method quantifies these differences as a function of both the stellar mass and the total cluster mass, and offers the advantage that it is insensitive to the exact functional form of the MF. We have applied our technique to completeness-corrected stellar mass functions in the range 0.25-0.75 $M_\odot$ for a sample of 27 globular clusters taken from the ACS Survey for GCs, and have com-

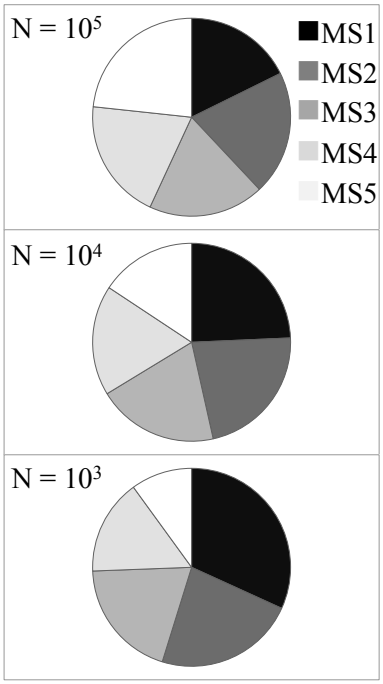

Figure 3. Stellar mass functions depicted in pie chart form. The total area of each circle corresponds to the total number of stars spanning all five stellar mass bins, and each pie slice shows the fraction of this total corresponding to each mass bin. Each of these fractions was calculated using the weighted lines of best-fit provided in Table 4. From top to bottom, the total number of stars used to generate each pie chart was 10^5, 10^4, and 10^3. Darker pie slices correspond to more massive bins. The sequence of pie charts progressing from top to bottom effectively shows the evolution of the stellar mass function with increasing dynamical age.

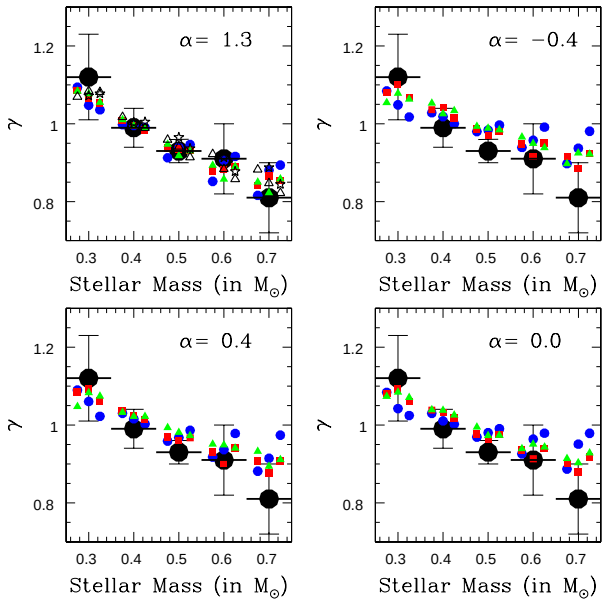

Figure 4. Comparison of the observed γ_i values to the corresponding model γ_i values for every combination of initial conditions. The observed γ_i's are shown as solid circles, whereas the model γ_i's are shown as different symbols. Each inset shows the model γ_i's for a different IMF. Starting at the upper right and rotating clockwise, the insets correspond to IMF slopes (in Equation 2) of -0.4, 0.0, 0.4, and 1.3. The online version of this plot shows the model γ_i's either as open or coloured symbols which have been used to indicate different initial concentrations. The solid blue circles, solid red squares, solid green triangles, open black triangles, and open five-point stars correspond to initial concentrations (W_0) of 5.0, 5.5, 6.0, 6.5, and 7.0, respectively. A small offset has been implemented for every stellar mass bin to indicate different initial virial radii, with the virial radius increasing from left to right. A horizontal line has also been included on every observed data point in order to indicate the width of the corresponding stellar mass bin.

pared the results to a series of Monte Carlo models for GC evolution.

In the subsequent sections, we discuss the implications of our results for the formation and evolution of Milky Way GCs.

4.1 The Effects of Two-Body Relaxation

We have shown that the observed differences in the present-day MFs in our sample can be reproduced by assuming (1) an universal initial mass function for all clusters, and (2) that internal two-body relaxation is the dominant mechanism contributing to the cluster-to-cluster variations.

Our results are the most reliable in the mass range 0.45 - 0.75 $M_\odot$. This is due to the larger photometric errors at the fainter magnitudes corresponding to lower stellar masses, and incompleteness resulting from crowding. Despite the high quality of the data used in this study, these issues are currently unavoidable given the nature of the observations. This will be a key challenge for future studies to resolve, however the method we have presented in this paper offers a robust means of performing future analyses. We note that the results of our observational analysis are consistent with those of De Marchi, Paresce & Portegies Zwart (2010), who fit a tapered power-law distribution function with an exponential truncation to the stellar mass functions of a sample of 30 clusters containing both young and old members. We have also verified that our results are consistent with those of Paust et al. (2010), who performed power-law fits to the MFs of 17 GCs taken from the ACS Survey.

In this paper, we have focused on the *local* MFs in the central cluster regions of the GCs in our sample. However, previous studies have shown that the *local* MF can differ considerably from the *global* MF (e.g. Vesperini & Heggie 1997). In principle, this should not have affected our comparisons between the observed and simulated MFs since we have considered the same structural areas of the clusters in all cases.

4.2 The Effects of Binary Stars

Binary stars are unresolved in GCs, appearing as single objects located above the MS in the cluster CMD. Therefore, we have included some objects in our number counts that are in fact binaries masquerading as single stars. Previous studies have shown that unresolved binaries can contribute to flattening, or even inverting, the stellar mass function in the range of stellar masses considered in this paper (e.g. Marks, Kroupa & Baumgardt 2008; Marks & Kroupa 2010). Moreover, observational evidence suggests that the binary fractions in GCs are inversely proportional to the total cluster mass (e.g. Sollima et al. 2008; Milone et al. 2008; Knigge, Leigh & Sills 2009). In particular, the most massive MW GCs tend to have binary fractions on the order of only a few percent (e.g. Rubenstein & Bailyn 1997; Cool et al. 2002; Davis et al. 2008), whereas the least massive MW GCs tend to have larger binary fractions that can even exceed 50% in some cases (e.g. Milone et al. 2011). This suggests that unresolved binaries should have had the largest effect on the MFs of the lowest mass clusters in our sample. Therefore, unresolved binaries could also be contributing to the general trend we have found of increasing γ_i with decreasing stellar mass.

In an effort to quantify the effects of unresolved binaries on our results, we removed all binaries from our simulated MFs and re-performed our weighted lines of best-fit. This confirmed that unresolved binaries could indeed be contributing to the general trend we have found of increasing γ_i with decreasing stellar mass. However, this effect was not significant in the models, in large part because we assumed a constant initial global binary fraction of 10% for all clusters. In order to reproduce the observed trend in γ_i, it would require that the range in binary fractions between low- and high-mass clusters is greater than the observed range by a factor $\gtrsim 2$ (e.g. Milone et al. 2011). Although the binary fractions generally increase in the core over time in our simulations (see Fregeau, Ivanova & Rasio (2009) for more details), they are not sufficiently high to have significantly contributed to the trend of increasing γ_i with decreasing stellar mass. At the end of our simulations, the core binary fractions are typically in the range 10-30%.

In order to properly assess these effects, objects that are in fact unresolved binaries should be identified and our analysis of the observations should be re-performed. This could be done using multi-band photometry since, if a given binary happens to fall on a single star evolution track in one CMD, it is unlikely to fall on the corresponding tracks in other CMDs constructed using different wavelength bands. Stellar evolution models could then be used to constrain the masses of the component stars. We intend to address this issue in future work.

We expect that the influence of binaries on GC evolution by, for example acting as heat-sources via hardening encounters with single stars (e.g. Hut & Bahcall 1983; Hut 1983; Fregeau, Ivanova & Rasio 2009), should have had a negligible impact on our results. This is because most of the clusters in our sample should still be undergoing core contraction (e.g. Gieles, Heggie & Zhao 2011). It follows that their central densities have not yet become sufficiently high for encounters involving binaries to occur frequently enough that they could have significantly affected the cluster evolution. Notwithstanding, future studies should incorporate models spanning a range of realistic initial binary fractions and distributions of orbital parameters in order to properly assess all of these effects.

4.3 The Effects of Tides from the Galaxy

Tides from the Galaxy effectively reduce the time-scale on which two-body relaxation operates (e.g. Heggie & Hut 2003). This primarily serves to make clusters appear more dynamically evolved than they otherwise would. The same effect is caused by disc shocking which, as with tidal effects, should most severely affect clusters with the lowest masses and the smallest Galactocentric distances. Therefore, the locations of clusters within their host galaxies has been shown to play an important role in determining the degree of flattening of their stellar MFs (e.g. Vesperini & Heggie 1997). In an effort to quantify the effects caused by tides on our observational results, we performed several cuts in perigalacticon distance and re-performed our weighted lines of best-fit. Estimates for the perigalacticon distances were obtained from Dinescu, Girard & van Altena (1999) and Casetti-Dinescu et al. (2007) for every cluster in our sample. Despite removing clusters with small perigalacticon distances for which it is typically argued that tidal effects should be the most severe (e.g. Heggie & Hut 2003), our lines of best-fit remained the same. We caution that these effects have not been fully accounted for in the simulations of GC evolution performed in this paper, for which we adopted circular orbits and a Galactocentric distance of 4 kpc in all cases. We intend to adopt a more realistic distribution of Galactic orbits for our model clusters in a future paper in order to properly assess the effects caused by tides in determining the present-day MFs of the GCs in our observed sample.

4.4 The Effects of Primordial Gas Expulsion

As discussed in Marks, Kroupa & Baumgardt (2008) and Marks & Kroupa (2010), the expulsion of primordial gas early on in the cluster lifetime can have a dramatic effect on the stellar MFs of clusters. In particular, these authors showed that clusters that began their lives with smaller concentrations are more likely to have lost a larger fraction of their low-mass stars as a result of this effect. Primordial gas expulsion could therefore contribute to improving the agreement we have found between the observed and simulated MFs. This would be accomplished if our γ_i values for the models were simultaneously increased for low stellar masses and decreased for high stellar masses, as is evident from Figure 4. This would occur if primordial gas expulsion had a more pronounced effect on the MFs of the lowest mass clusters in our sample. This is not unreasonable since the depth of the cluster potential increases with increasing cluster mass.

4.5 Future Work

Given the very old ages and therefore low metallicities ([Fe/H] $\approx$ -2.28 - (-0.37)) of the clusters in our sample, our technique could potentially be used to better constrain the

IMFs of old massive star clusters and, more generally, star formation in the very early Universe. This will be done in a forthcoming paper by considering a larger range of IMFs and initial cluster conditions than we have considered here.

Finally, we wish to point out that the method we have presented can be generalized to compare any large sample of distribution functions. We intend to illustrate this in a future paper by using our technique to quantify cluster-to-cluster differences in the orbital distributions (period, eccentricity, and mass-ratio) of the binary populations in GCs as a function of the total cluster mass.

ACKNOWLEDGMENTS

We would like to thank an anonymous referee for several suggestions that helped to improve our manuscript. We also wish to thank Christopher McKee for useful discussions, Aaron Dotter and Roger Cohen for their support in analyzing the observations, and Robert Cockcroft for a critical read of our manuscript. N.L. was supported by Ontario Graduate Scholarships (OGS) and the European Space Agency (ESA). S.U. was supported by NSF Grant AST-0607498 and NASA ATP Grant NNX09AO36G at Northwestern University.

REFERENCES

Anderson J., King I. R., Richer H. B., Fahlman G. G., Hansen B. M. S., Hurley J., Kalirai J. S., Rich R. M., Stetson P. B. 2008, AJ, 135, 2114
Baumgardt H., Makino J. 2003, MNRAS, 340, 227
Baumgardt H., De Marchi G., Kroupa P. 2008, ApJ, 685, 247
Bonnell I. A., Larson R. B., Zinnecker H. 2007, Protostars and Planets V, ed. B. Reipurth, D. Jewitt, & K. Keil (Tucson: University of Arizona Press), 951, 149
Chatterjee S., Fregeau J. M., Umbreit S., Rasio F. A. 2010, ApJ, 719, 915
Chernoff D. F., Weinberg M. D. 1990, ApJ, 351, 121
Cool A. M., Bolton A. S. 2002, in ASP Conference Series 263, Stellar Collisions, Mergers and their Consequences, ed. M. M. Shara (San Francisco: Astronomy Society of the Pacific), 163
Da Costa G. S. 1982, AJ, 87, 990
Davis D. S., Richer H. B., Anderson J., Brewer J., Hurley J., Kalirai J. S., Rich R. M., Stetson P. B. 2008, AJ, 135, 2155
Dinescu D. I., Girard T. M., van Altena W. F. 1999, AJ, 117, 1792
Casetti-Dinescu D. I., Girard T. M., Herrera D., van Altena W. F., Lopez C. E., Castillo D. J. 2007, AJ, 134, 195
De Angeli F., Piotto G., Cassisi S., Busso G., Recio-Blanco A., Salaris M., Aparicio A., Rosenberg A. 2005, AJ, 130, 116
De Marchi G., Paresce F., Pulone L. 2007, ApJ, 656, L65
De Marchi G., Paresce F., Portegies Zwart S. 2010, ApJ, 718, 105
Dotter A., Chaboyer B., Jevremovic D., Baron E., Ferguson J. W., Sarajedini A., Anderson J. 2007, AJ, 134, 376
Dotter, A., Sarajedini A., Anderson J., Aparicio A., Bedin L. R., Chaboyer B., Majewski S., Marin-Franch A., Milone A., Paust N., Piotto G., Reid N., Rosenberg A., Siegel M. 2010, ApJ, 708, 698
Elmegreen B. G. 1999, ApJ, 527, 266
Elmegreen B. G. 2001, ASP Conference Series 243: From Darkness to Light: Origin and Evolution of Young Stellar Clusters, ed. T. Montmerle & P. Andr (San Francisco: Astronomical Society of the Pacific), 243, 255
Fregeau J. M., Gurkan M. A., Joshi K. J., Rasio F. A. 2003, ApJ, 593, 772
Fregeau J. M., Rasio F. A. 2007, ApJ, 658, 1047
Fregeau J. M., Ivanova N., Rasio F. A. 2009, ApJ, 707, 1533
Gieles M., Heggie D., Zhao H. 2011, MNRAS, 413, 2509
Goldsbury R., Richer H. B., Anderson J., Dotter A., Sarajedini A., Woodley K. 2010, AJ, 140, 1830
Grenier I. A., Casandjian J. M., Terrier R. 2005, Science, 307, 1292
Harris, W. E. 1996, AJ, 112, 1487 (2010 update)
Heggie D. C., Giersz M. 2008, MNRAS, 389, 1858
Heggie D. C., Giersz M. 2009, MNRAS, 397, 46
Heggie D. C., Hut P. 2003, The Gravitational Million-Body Problem: A Multidisciplinary Approach to Star Cluster Dynamics (Cambridge: Cambridge University Press)
Henon M. 1960, Annales d'Astrophysique, 23, 668
Henon M. 1973, Dynamical Structure and Evolution of Dense Stellar Systems, ed. L. Martinet & M. Mayor (Sauverny: Observatoire de Geneve), 183
Hurley, J. R., Pols, O. R., Aarseth, S. J. & Tout, C. A. 2005, MNRAS, 363, 293
Hut P., Bahcall J. N. 1983, ApJ, 268, 319
Hut P. 1983, ApJ, 272, 29
Joshi K. J., Rasio F. A., Portegies Zwart S. 2000, ApJ, 540, 969
Joshi K. J., Nave C. P., Rasio F. A. 2001, ApJ, 550, 691
Knigge C., Leigh N., Sills A. 2009, Nature, 457, 288
Kroupa P. 2001, MNRAS, 322, 231
Kroupa P., Weidner C., Pflamm-Altenburg J., Thies I., Dabringhausen J., Marks M., Maschberger T. 2011, arXiv:1112.3340
Kruijssen J. M. D., Mieske S. 2009, A&A, 500, 785
Lada C. J. 1985, ARA&A, 23, 267
Lada E. A., Lada C. J. 1995, AJ, 109, 1682
Lada C. J., Lada E. A. 2003, ARA&A, 41, 57
Lada C. J., Alves J. F., Lombardi M. 2007, Protostars and Planets V, ed. B. Reipurth, D. Jewitt, & K. Keil (Tucson: University of Arizona Press), 951, 3
Leigh N., Sills A., Knigge C. 2011, MNRAS, 415, 377
Lejeune Th., Cuisinier F., Buser R. 1997, A&AS, 125, 229
Lejeune Th., Cuisinier F., Buser R. 1998, A&AS, 130, 65
Marin-Franch A., Aparicio A., Piotto G., Rosenberg A., Chaboyer B., Sarajedini A., Siegel M., Anderson J., Bedin L. R., Dotter A., Hempel M., King I., Majewski S., Milone A. P., Paust N., Reid I. N. 2009, ApJ, 694, 1498
Marks M., Kroupa P., Baumgardt H. 2008, MNRAS, 386, 2047
Marks M., Kroupa P. 2010, MNRAS, 406, 2000
McKee C. F., Ostriker E. C. 2007, ARA&A, 45, 565
Milone A. P., Piotto G., Bedin L. R., Sarajedini A. 2008, MmSAI, 79, 623
Milone A. P., Piotto G., Bedin L. R., Aparicio A., Anderson J., Sarajedini A., Moretti A., Davies M. B., Chaboyer B., Dotter A., Hempel M., Marin-Franch A., Majewski S.,

Paust N. E. Q., Reid I. N., Rosenberg A., Siegel M. 2011, A&A, in press (arXiv:1111.0552)
Murray N. 2009, ApJ, 691, 946
Parravano A., McKee C. F., Hollenbach D. J. 2011, ApJ, 726, 27
Paust N. E., Reid I. N., Piotto G., Aparicio A., Anderson J., Sarajedini A., Bedin L. R., Chaboyer B., Dotter A., Hempel M., Majewski S., Marin-Franch A., Milone A., Rosenberg A., Siegel M. 2010, AJ, 139, 476
Pols O. R., Schroder K.-P., Hurley J. R., Tout C. A., Eggleton P. P. 1998, MNRAS, 298, 525
Portegies Zwart S. F., McMillan S. L. W., Hut P., Makino J. 2001, MNRAS, 321, 199
Portegies Zwart S. F., McMillan S. L. W., Gieles M. 2010, ARA&A, 48, 431
Rubenstein E. P., Bailyn C. D. 1997, ApJ, 474, 701
Sarajedini A., Bedin L. R., Chaboyer B., Dotter A., Siegel M., Anderson J., Aparicio A., King I., Majewski S., Marin-Franch A., Piotto G., Reid I. N., Rosenberg A., Steven M. 2007, AJ, 133, 1658
Scalo J. 1998, ASP Conference Series 142: The Stellar Initial Mass Function (38th Herstmonceux Conference), ed. G. Gilmore & D. Howell (San Francisco: Astronomy Society of the Pacific), 142, 201
Sollima A., Beccari G., Ferraro F. R., Fusi Pecci F., Sarajedini A. 2007, A&A, 481, 701
Spitzer L. 1987, Dynamical Evolution of Globular Clusters (Princeton: Princeton University Press)
Tutukov A. V. 1978, A&A, 70, 57
Vesperini E., Heggie D. C. 1997, MNRAS, 289, 898
von Hippel T., Sarajedini A. 1998, AJ, 116, 1789
Zonoozi A. H., Kupper A. H. W., Baumgardt H., Haghi H., Kroupa P., Hilker M. 2011, MNRAS, 411, 1989

This paper has been typeset from a TEX/ LATEX file prepared by the author.